Available online at www.sciencedirect.com
ScienceDirect
Journal of the European Ceramic Society 30 (2010) 1229–1236
www.elsevier.com/locate/jeurceramsoc

# First- and second-order approaches for the direct determination of bridging stresses from R-curves

S. Fünfschilling [a,*], T. Fett [a], S.E. Gallops [b], J.J. Kruzic [b], R. Oberacker [a], M.J. Hoffmann [a]

[a] *Universität Karlsruhe, Institut für Keramik im Maschinenbau, 76131 Karlsruhe, Germany*
[b] *Materials Science, School of Mechanical, Industrial, and Manufacturing Engineering, Oregon State University, USA*

Received 15 May 2009; received in revised form 5 November 2009; accepted 26 November 2009
Available online 31 December 2009

**Abstract**

A procedure is presented that allows the simple estimation of bridging stresses from crack growth resistance curve (R-curve) data. The first-order approximation results by taking the derivative of the R-curve. For an increased degree of accuracy a second-order solution is suggested. This step includes straight-forward integration of the first-order results. The procedure is outlined in detail and applied to fatigue threshold R-curve results for a $MgO + Y_2O_3$-doped silicon nitride (MgY-SN) and an 99.5% pure alumina obtained with compact tension specimens, and fracture toughness R-curve results for a $MgO + La_2O_3$-doped silicon nitride (MgLa-SN) obtained with notched bending bars. The approximate bridging stresses are compared with the "full solutions" computed with much more effort by solving a system of integral equations.


*Keywords:* Alumina; Crack-face bridging; Crack-tip toughness; R-curve; Silicon nitride

## 1. Introduction

The increasing crack resistance of ceramic materials is of high interest for technical applications. Crack growth resistance curve (R-curve) behaviour is commonly described by a relation $K_R = f(\Delta a)$ in which $K_R$ is the stress intensity factor necessary for crack propagation by an amount of $\Delta a$ (Fig. 1). This would be an appropriate description for the case if the R-curves were pure material properties. However, it has been shown by experimental and theoretical investigations that the R-curve is not a unique material property. R-curves for naturally small cracks are often different from those for macroscopic cracks. A survey of data is given by Munz[1] that show the trend of lower R-curves for small natural cracks.

So far it is the common opinion that in the special case of R-curves caused by grain bridging effects, the relation between the bridging stresses and crack opening displacement, $\sigma_{br} = f(\delta)$, is the intrinsic material property which is expected to be unaffected by test conditions such as the geometry of the test specimen or the type of loading (tension, bending, etc.). This assumption is true for case of disappearing or negligible T-stresses as outlined in Ref. 2.

Direct measurements of the loads transferred by the bridges were performed by Pezzotti et al.[3,4] and Kruzic et al.[5] applying Raman spectroscopy. Another popular method to determine the bridging stress relation is the evaluation of crack opening displacement (COD) measurements, as used in Ref. 6. Finally, Fett et al. have developed a method for determining the bridging stress relation directly from the R-curve[7]; however, the exact approach requires the solution of a system of simultaneous integral equations in Ref. 7 that needs much numerical effort. This motivates developing approximate relations from which at least the near-tip bridging behaviour can be determined. Thus, in this paper a straight-forward method for the determination of bridging stresses from R-curves is proposed and compared to results given by the exact method of Ref. 7.

## 2. Determination of bridging stresses from R-curves

### 2.1. Basic relations

A procedure that allows the bridging stresses to be determined from existing R-curve results was developed in Ref. 7. From the measured R-curves the bridging stress intensity factor, $K_{br}$, can

* Corresponding author. Tel.: +49 721 608 7925; fax: +49 721 608 8891.
*E-mail address:* stefan.fuenfschilling@kit.edu (S. Fünfschilling).

0955-2219/$ – see front matter © 2009 Elsevier Ltd. All rights reserved.
doi:10.1016/j.jeurceramsoc.2009.11.013

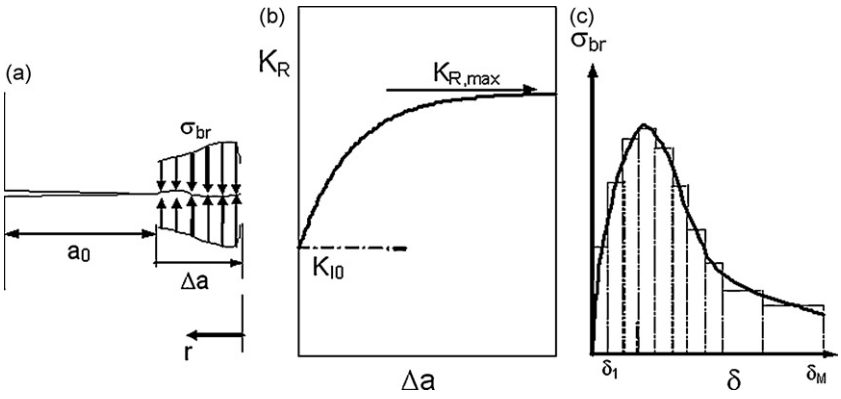


Fig. 1. (a) A crack in a ceramic material exhibiting crack surface interactions by bridging stresses, (b) schematic of an increasing crack growth resistance curve starting from the crack-tip toughness $K_{I0}$ with a rather linear increase and exhibiting a saturation value $K_{R,\max}$, and (c) bridging stress versus crack opening displacement $\delta$ with representation by a histogram of $M$ stress values.

be determined since:

$$K_R = K_{I0} - K_{br}, \quad K_{br} < 0, \tag{1}$$

($K_{I0}$ = crack-tip toughness). The necessary procedures are extensively outlined in the literature. For our purposes we mostly used the technique described in Ref. 7.

Using the weight function representation, the bridging stress intensity factor can be represented by the distribution of bridging stresses, $\sigma_{br}$, acting in the wake of the crack as given by:

$$K_{br}(\Delta a) = \int_{a_0}^{a_0+\Delta a} h(r,a)\sigma_{br}(\delta(r,a))dr, \tag{2}$$

where $h$ is fracture mechanics weight function, $r$ is the distance from the tip, $a_0$ is the initial crack length free of bridging, and $\Delta a = a - a_0$ is the crack extension (Fig. 1a). The bridging stresses depend on the actual crack opening displacements, $\delta$.

The total displacements in the presence of bridging stresses result from:

$$\delta = \delta_{appl} + \delta_{br},$$
$$\delta_{br} = \frac{1}{E'}\int_{a-r}^{a} h(r,a')da' \int_0^{a'} h(r',a')\sigma_{br}(\delta(r',a))dr', \tag{3}$$

with the plane strain modulus $E' = E/(1-\nu^2)$ and the "applied displacements" (the displacements under the same load in the absence of the bridging stresses):

$$\delta_{appl} = \frac{1}{E'}\int_{a-r}^{a} h(r,a')K_{appl}(a')da'. \tag{4}$$

The applied stress intensity factor, $K_{appl}$, is given in fracture mechanics handbooks for various test specimens.

The system of Eqs. (2) and (3) can be solved by "successive approximation", starting with an (in principle) arbitrary first approximation of the bridging relation, $\sigma_{br}(\delta)$, for instance given by a histogram of $M$ bridging stresses $\sigma_{br}(\delta_1), \ldots, \sigma_{br}(\delta_M)$ as illustrated in Fig. 1c. As the starting value for the displacements, the applied crack opening displacement field $\delta = \delta_{appl}$ may be used, resulting in the first distribution of the bridging stresses $\sigma_{br} = f(\delta_{appl}(r,a))$. These stresses must then be introduced under the integral of (3), yielding an improved distribution of the total displacements, $\delta$, and an improved bridging stress distribution. After a few iteration steps the solution of (3) will converge as long as the first approximation for the bridging law has not been chosen to be too unrealistic. This procedure must be repeated for a number of $N \geq M$ crack lengths $a_1, \ldots, a_N$. For these crack lengths the bridging stress intensity factors $K_{br}(a_1), \ldots, K_{br}(a_N)$ must be computed from (2) and the related $K_R$-values from (1).

This iterative solution may establish the inner loop of a computer program. In the outer loop the bridging law, $\sigma_{br}(\delta)$, has to be changed systematically (by application of an optimization procedure, e.g., Ref. 8) until the computed and the measured $K_R$ are identical at all chosen crack lengths if $N = M$ or in a least-squares sense if $N > M$.

It has to be emphasized that the procedures for solving the system of Eqs. (2) and (3) need much numerical effort, especially for large numbers $M$ and $N$, and require some experience.

### 2.2. Approximate solutions

By taking the derivative with respect to $a$ on both sides of (2) the result is:

$$\frac{dK_{br}}{da} = -\frac{dK_R}{da} = h(r,a)\sigma(r,a)|_{r=\Delta a} + \int_{a_0}^{a}\frac{\partial h(r,a)}{\partial a}\sigma_{br}(r,a)dr + \int_{a_0}^{a} h(r,a)\frac{\partial \sigma_{br}(r,a)}{\partial a}dr. \tag{5}$$

The bridging stresses are then given as:

$$\sigma_{br}|_{r=\Delta a} = -\frac{1}{h|_{r=\Delta a}}\frac{dK_R}{da} - \frac{1}{h|_{r=\Delta a}}\int_{a_0}^{a}\frac{\partial h(r,a)}{\partial a}\sigma_{br}(r,a,\Delta a)dr - \frac{1}{h|_{r=\Delta a}}\int_{a_0}^{a} h(r,a)\frac{\partial \sigma_{br}(r,a,\Delta a)}{\partial a}dr. \tag{6}$$

Identifying $\sigma_{br}(r) = \sigma_{br}|_{r=}\,\Delta a$ gives a *first-order solution* for the bridging stresses:

$$\sigma_{br}^{(1)}(r) = -\frac{1}{h}\frac{dK_R}{da}\bigg|_{\Delta a = r}. \tag{7}$$

In the first-order approximation, only the first term of Eq. (6) was regarded with the bridging stresses depending exclu-

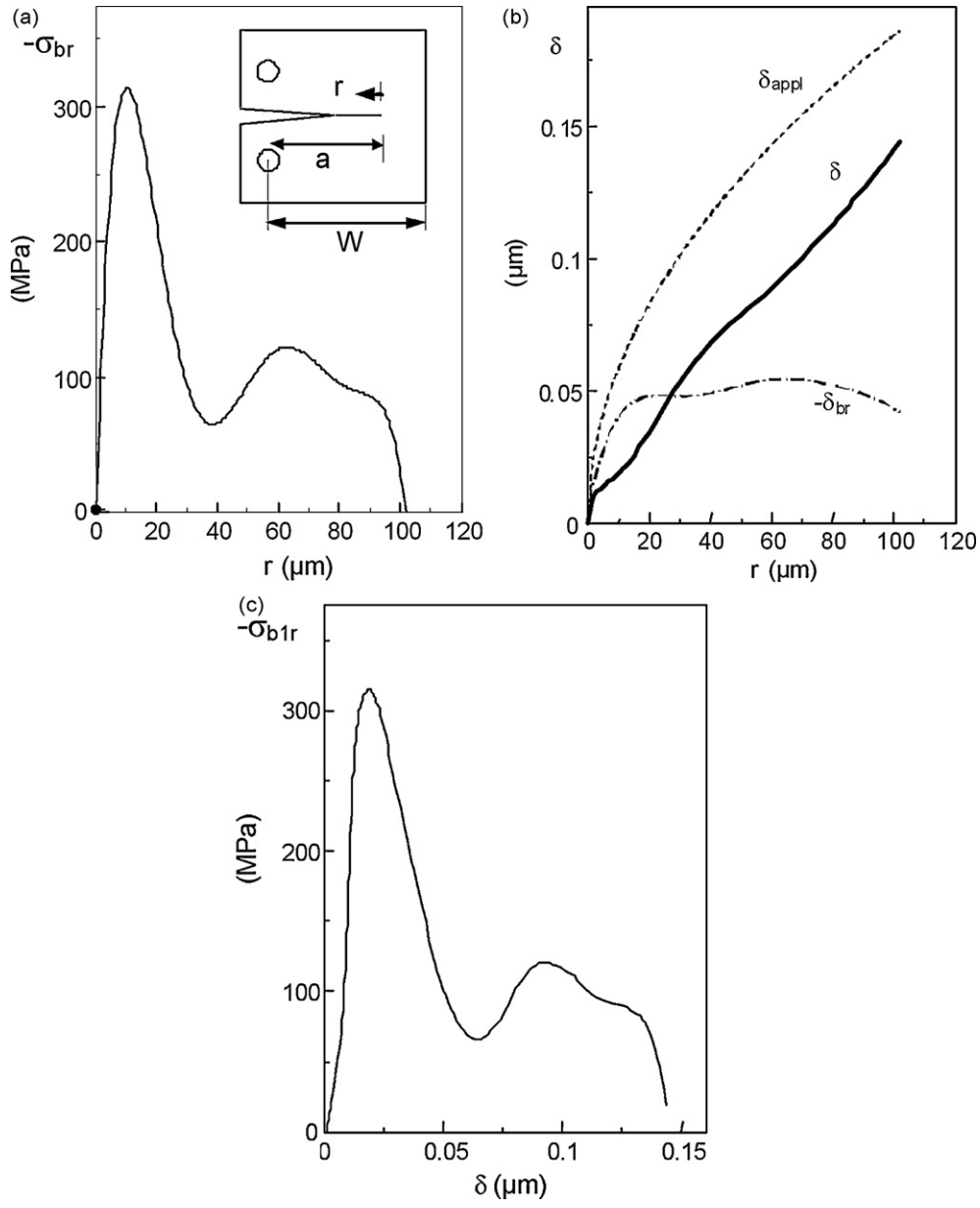


Fig. 2. For MgY-SN: (a) bridging stress distribution from Ref. 5, (b) computation of the total displacements $\delta$, composed of the applied displacements, $\delta_{appl}$, and the bridging displacements, $\delta_{br}$, and (c) "bridging law" obtained by combining parts (a) and (b).

sively on $r$. In a second-order solution, the first integral term of (6) accounting for the influence of crack length via the weight function $h(r, a)$ may be included. In this approximation, the first-order solution (7) is used under the integral, resulting in:

$$\sigma_{br}^{(2,1)}(r) = \sigma_{br}^{(1)}(r) - \frac{1}{h|_{r=\Delta a}} \int_{a_0}^{a} \frac{\partial h(r,a)}{\partial a} \sigma_{br}^{(1)}(r) dr. \quad (8)$$

where the first number in the superscript indicates that up to, and including, the second term of (6) is used in the approximation, and the second number gives the step of iteration (started with $m = 1$). Generally it holds for higher iteration numbers $m > 1$:

$$\sigma_{br}^{(2,m)}(r) = \sigma_{br}^{(1)}(r) - \frac{1}{h|_{r=\Delta a}} \int_{a_0}^{a} \frac{\partial h(r,a)}{\partial a} \sigma_{br}^{(2,m-1)}(r) dr. \quad (9)$$

## 3. Evaluation of approximation methods using experimental results

The purpose of this section is to assess the capability of the first- and second-order approximations to yield results near in accuracy to the exact method from Ref. 7. Furthermore, one simplifying assumption commonly made is to calculate R-curves, $K_R(\Delta a)$, directly from the measured bridging stress distribution, $\sigma_{br}(r)$, rather than the intrinsic material property, $\sigma_{br}(\delta)$, by assuming that the crack opening profile, $\delta(r)$, is independent of crack size over the relevant range of $\Delta a$. Accordingly, the approximation methods are compared to the full method of Ref. 7 for ceramics with very different bridging behaviours ($Si_3N_4$ and $Al_2O_3$), while possible errors introduced by the assumption in Ref. 5 are also assessed.

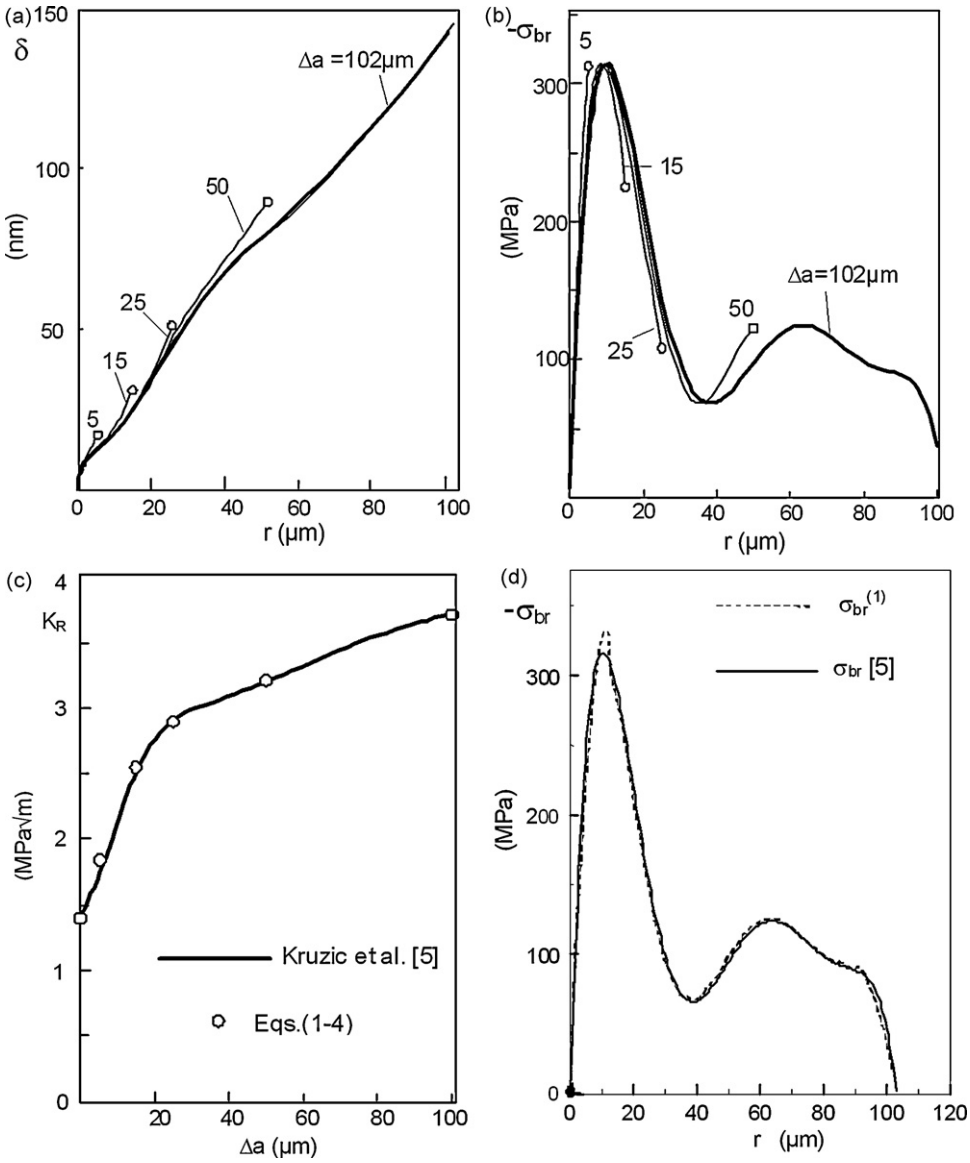


Fig. 3. For MgY-SN: (a) total displacement profiles for shorter crack extension phases, (b) bridging stress distribution for these cracks, (c) R-curve, in terms of $K_{max}$, calculated from the bridging stresses in (b) shown as the circles while the solid curve is that calculated by Kruzic et al.,[5] and (d) first-order solution for the bridging stresses (dashed curve) resulting from the computed R-curve by application of Eq. (7) compared with the input stress distribution of Fig. 2a (solid curve).

### 3.1. Application to cracks in CT-specimen specimens

#### 3.1.1. Silicon nitride

In Ref. 5, Kruzic et al. reported a bridging stress distribution, $\sigma_{br}(r)$, in a MgO and $Y_2O_3$ containing silicon nitride (MgY-SN) measured using Raman spectroscopy (Fig. 2a). The measurements were made using a compact tension (CT) specimen with width $W = 19$ mm, $a_0 = 6.5$ mm, and $a = 12.5$ mm. The crack was grown by fatigue cycling using sine wave cyclic loading at 25 Hz with a constant load ratio of $P_{min}/P_{max} = R = 0.1$. Fatigue thresholds were determined by reducing the applied stress intensity range, $\Delta K = K_{max} - K_{min}$, at a constant $\Delta K$ gradient:

$$\nabla = \frac{1}{\Delta K}\left(\frac{d\Delta K}{da}\right), \tag{10}$$

equal to −0.08/mm until the crack growth rate slowed to approximately $10^{-10}$ m/cycle, which is experimentally defined as the fatigue threshold. $K_{max}$ and $K_{min}$ are the maximum and minimum applied stress intensities during the loading cycle, respectively. By Raman spectroscopy, it was found that the bridging stresses approached zero roughly 100 μm behind the crack-tip, thus measurements ceased after that point. Due to cyclic degradation of the bridges, these measured bridging stresses are of course lower than those from a test under monotonously rising load. Using a sixth-order polynomial fit to the measured stress data, a fatigue threshold R-curve, $K_R(\Delta a)$, was calculated over ∼100 μm until a plateau was assumed where $\sigma_{br}(r)$ approached zero.

In Ref. 5, two numerical results were reported which both would be an appropriate input for a sensitivity study. An attempt using both numerical data sets, namely the calculated $K_R(\Delta a)$

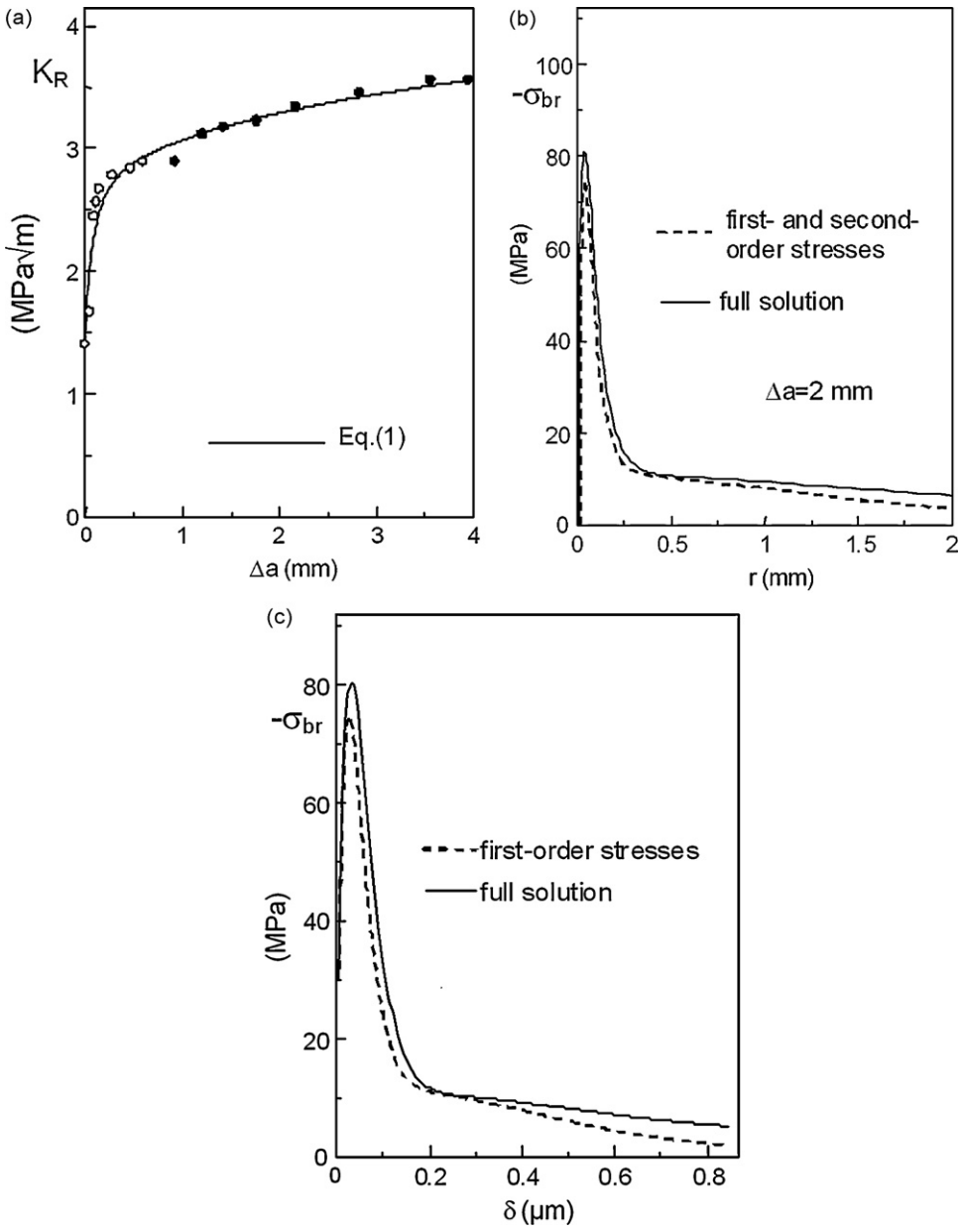


Fig. 4. For $Al_2O_3$: (a) measured R-curve data, in terms of $K_{max}$, where each symbol represents an individual sample and the line represents the fit to Eq. (11), (b) first-order bridging stresses compared with the full solution, and (c) the related bridging laws.

*and* polynomial fit of the $\sigma_{br}(r)$ data, as the input is not recommendable because it establishes a clearly overdetermined problem. In order to assess the accuracy of the mathematical procedure, we needed to avoid the influence of numerical data from different representations. Since the R-curve in Ref. 5 was computed from the bridging stresses, those stresses are used as the basis to assess the influence of the constant crack opening profile assumption in Ref. 5 on the results. The fact that $\sigma_{br}(r)$ comes from Raman-measurements with rather large scatter is without any relevance for the following considerations since any arbitrarily given distribution can be used for this purpose.

The stress field, $\sigma_{br}(r)$, expressed by a polynomial of 6th degree with respect to the crack-tip distance, $r$, was introduced into Eq. (3) resulting in the total displacements, $\delta(r)$ (Fig. 2b). The stress polynomial, $\sigma_{br}(r)$, in combination with the total displacements, $\delta(r)$, establishes the complete bridging law, $\sigma_{br}(\delta)$, as shown in Fig. 2c. Based on this relation, it is possible to compute the total crack opening displacements for any crack with increments of $0 < \Delta a \leq 102$ μm. Some results are shown in Fig. 3.

Fig. 3a represents the calculated displacement profiles for four cracks with extensions shorter than the bridging zone size. From these profiles and the bridging law, the individual bridging stress distributions are obtained (Fig. 3b). From Eq. (2), the related bridging stress intensity factors were determined and via Eq. (1) the R-curve data, $K_R(\Delta a)$, were calculated as shown in Fig. 3c by the circles. Note, the points calculated using the full solution taking into account the exact $\delta(r)$ for each crack size agree almost exactly with the R-curve calculated in Ref. 5 using the simplifying assumption that $\delta(r)$ is the same for both long and

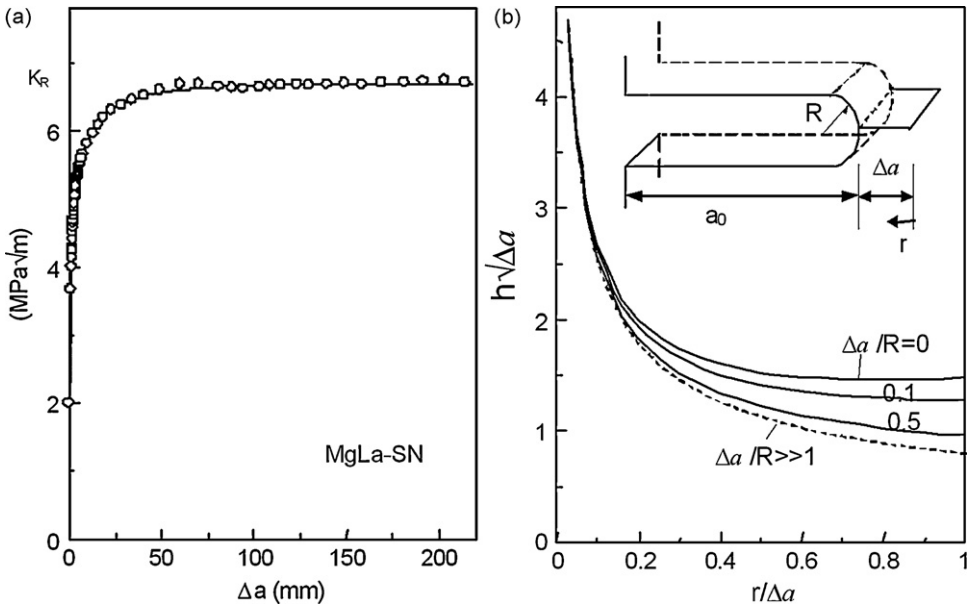


Fig. 5. For MgLa-SN: (a) R-curve (symbols measurements, curve: fitted according to Eq. (11)) and (b) weight function for a crack ahead of a slender notch.

short cracks. The R-curve calculated in Ref. 5, which is shown as a solid line, is given by interpolating 17 data pairs ($K_R$, $\Delta a$) by cubic splines.

Since the R-curve calculated in Ref. 5 was deemed accurate, it was then used to demonstrate the ability of the first-order approximation to accurately reflect the exact solution method. The first-order bridging stresses were determined by use of Eq. (7) and introduced in Fig. 3d as the dashed curve. This is essentially the reverse calculation of that described above, but using the first-order approximation instead of the full method of Ref. 7. Comparison of this result with the input stress distribution of Fig. 2a, introduced in Fig. 3d by the solid curve, shows a very good agreement. A second-order evaluation of the R-curve according to Eq. (9) with ($n=2$, $m=1$) showed deviations from the first-order solution less than 0.15 MPa. Therefore, this result is not plotted in Fig. 3d.

### 3.1.2. Alumina

Fatigue threshold R-curve measurements were carried out on two CT-specimens (width $W=19.2$ mm and thickness $B=3.5$ mm) of 99.5% pure $Al_2O_3$. The grain diameters were widely distributed, with a mean lineal intercept of ~1.7 μm and individual grain diameters ranging from sub-micrometer to >25 μm. Fatigue cracks were initiated from machined notches ($a_0=5.8$ mm) that were sharpened by razor micronotching to root radii $\rho<10$ μm. Fatigue testing was conducted as described for $Si_3N_4$, except that the fatigue threshold was recorded at successively increasing crack lengths by step increasing the load after each measurement, resulting in the data shown in Fig. 4a where $K_R$ is given in terms of $K_{max}$. The best fit of these data was given by:

$$K_R = K_{I0} + C_1(1-(1+C_2\sqrt{\Delta a})\exp[-C_2\sqrt{\Delta a}]) + C_3(1-(1+C_4\sqrt{\Delta a})\exp[-C_4\sqrt{\Delta a}]) \quad (11)$$

with the "best" set of coefficients:

$$C_1 = 1.305\,\text{MPa}\sqrt{\text{m}},\quad C_2 = 237.3/\sqrt{\text{m}},$$
$$C3 = 1.523\,\text{MPa}\sqrt{\text{m}},\quad C_4 = 29.67/\sqrt{\text{m}},$$

represented in Fig. 4a by the curve.

Application of Eq. (7) on the fit relation (11) yields the bridging stresses as shown in Fig. 4b as the dashed curve. The difference between the first- and second-order approximations was less than 1 MPa. Therefore, the two results were represented in Fig. 4b by one single dashed curve. The full solution obtained from the solution of the system of integral equations ((2) and (3)) with a much higher effort is plotted as the solid curve. Fig. 4c shows the related bridging laws. For the tested alumina the first-order approximation shows some deviations especially for the for the large crack-tip distances of $\Delta a>1$ mm.

### 3.2. Cracks emanating from notches in $Si_3N_4$ bending bars

For more complicated cracks with more complicated weight functions, such as a crack starting from a notch, the solutions of (7) and (9) need slightly increased effort.

An traditional fracture R-curve for a MgO and $La_2O_3$ containing silicon nitride (MgLa-SN) is shown in Fig. 5a. The test was carried out on a pre-notched bending bar. Procedures were identical to those found in Ref. 9, but briefly 4 point bend beams (3 mm × 4 mm × 25 mm) with razor micronotches ($\rho\approx 9.5$ μm) and 2.6 mm notch depth were loaded in displacement control until the onset of cracking. Crack lengths were monitored with an optical microscope. Load and displacement data where used to calculate the very first part of the R-curve.

For the determination of the bridging stresses, the weight function for a small crack ahead of a slender notch must be applied. It is given in Ref. 10 and can be written for the special case of a small crack extension compared to the initial crack

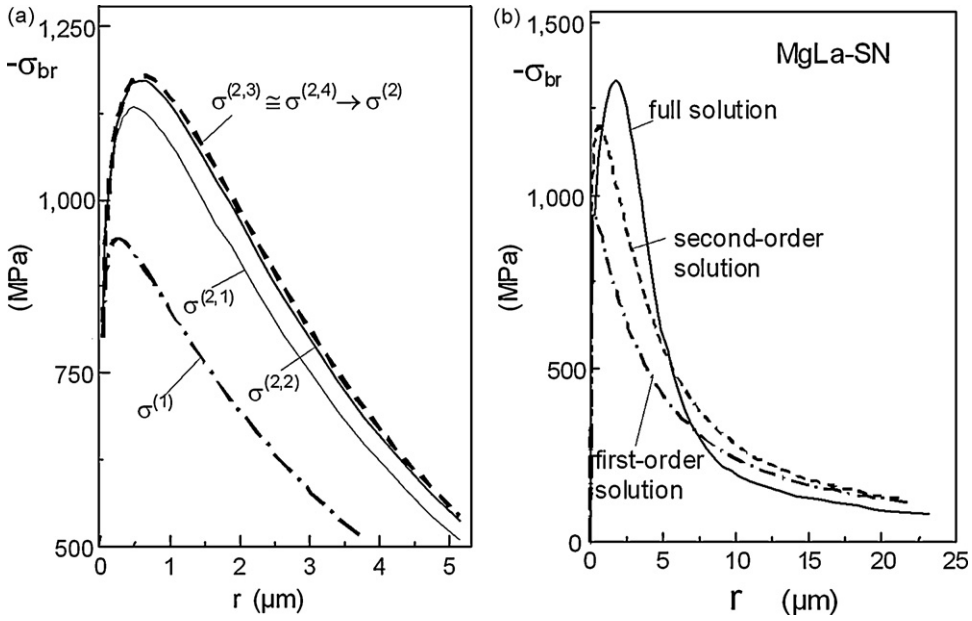


Fig. 6. For MgLa-SN: (a) convergence study of the second-order approximation and (b) first- and second-order bridging stresses compared with the full solution obtained by simultaneous solving the integral Eqs. (2) and (3).

length, $a - a_0 = \Delta a \ll a_0$

$$h_{notch} = \sqrt{\frac{2}{\pi \Delta a}} \left[ \frac{1}{\sqrt{r/\Delta a}} + 0.568\lambda \left( \sqrt{\frac{r}{\Delta a}} + \frac{1}{2} \left( \frac{r}{\Delta a} \right)^{3/2} \right) \right], \tag{12a}$$

with

$$\lambda = \left( \frac{R}{R + \Delta a} \right)^{7/2} \tag{12b}$$

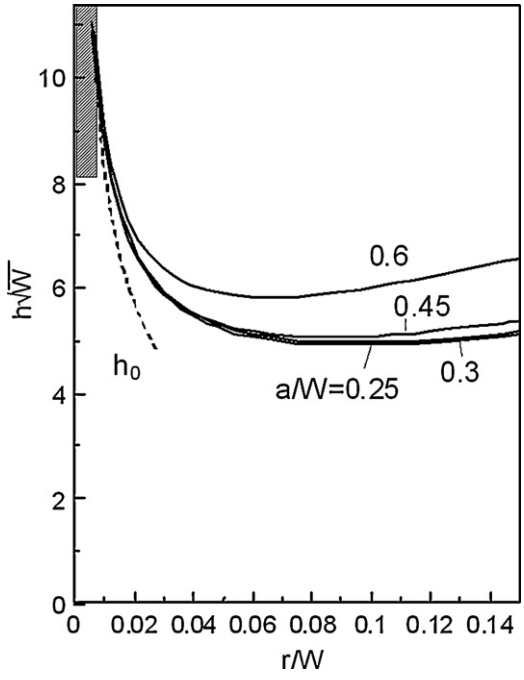


Fig. 7. Influence of the crack length a on the weight function for the CT-specimens; the hatched regions for $r/W < 0.007$ indicate the experiments by Kruzic et al.[5]

Fig. 5b shows this solution together with the geometric data $R$, $\Delta a$, and $r$. For very short crack extensions on the order of about $\Delta a \leq R$, the weight function significantly depends on $\Delta a/R$.

Application of Eq. (7) yields the first-order bridging stresses as represented in Fig. 6a by the dash-dotted curve. The first and second iterative solutions of Eq. (9) are given by the continuous curves. The third and fourth iterations showed differences less than 2 MPa, therefore, they are represented by the same dashed curve. This curve indicates the final curve of convergence, i.e. the bridging stress distribution $\sigma_{br}(r)$.

The full solution obtained by solving the simultaneous system of integral equations (2) and (3) is given in Fig. 6b by the solid curve. Although differences in the approximations exist, the second-order solution clearly exhibits all characteristic features of the exact solution, which are in this case very high bridging stresses of $\sigma_{br} \approx 1250$ MPa and a strong concentration of the bridging effects in a crack-tip distance of about $r = 0$–$10$ μm.

## 4. Discussion

Based on the evaluation of data for there different ceramics tested using two different specimen types, the following observations are made:

- The first- and second-order evaluations of the bridging stresses for the MgY-SN ceramic tested with the CT-specimen showed excellent agreement with the input stress data.
- For the $Al_2O_3$ ceramic with a much larger bridging zone size, also obtained with the CT-specimen, the difference of the approximate solutions from the full solution was still rather small.
- In contrast to these results, the MgLa-SN with a very steep R-curve tested with a notched bending bar showed clearly larger differences from the full solution.

- Only in the third example is the benefit of a second-order approximation evident; indeed, the addition of the second term was negligible for the first two cases.

These differences may be discussed by the following considerations.

The good agreement of the approximations in Fig. 3d is not really astonishing as can be concluded from Fig. 7. This diagram shows that the weight function $h(r/W, a/W)$ given in Ref. 10 is nearly independent of the relative crack length in the range $0.25 \leq a/W \leq 0.45$. The region of interest corresponds to a ratio of $r/W \leq 0.007$. In Fig. 7, this region is indicated by the hatched area. It is clearly visible that for such a small bridging zone the weight function is independent of the relative crack length. The derivative of the weight function with respect to crack length therefore disappears and an agreement between the first and second-order solutions becomes evident. This situation also allows the assumption in Ref. 5 regarding the crack opening displacements to be valid. In contrast, the $r/W$ values are much higher for the alumina examined due to the large bridging zone, causing a source of error, especially at large crack-tip distances. Finally, for the notched bend sample the weight function changes rapidly, even at short crack extensions, causing significant errors in the first and second-order solutions, although they do capture the general feature of the exact solution.

## 5. Summary

Simple first- and second-order approximations of bridging stresses have been derived that need only differentiation of the R-curve (first-order) and integrations (second-order). As examples of application, the bridging stresses for "fatigue threshold R-curves" on MgY-SN and $Al_2O_3$ obtained with CT-specimens are evaluated. It has been shown that a nearly exact solution of the bridging stresses can be achieved with relatively simple calculations for materials where the bridging zone is small compared to the specimen width (e.g., $Si_3N_4$ and SiAlON ceramics) and where the sample geometry is such that the weight function changes weakly at small crack extensions (e.g., CT-specimen). However, even with the CT-specimen caution must be taken as the bridging zone size becomes larger (e.g., $r/W > .01$), especially as the crack size becomes large ($a/W > 0.45$). Results for alumina show the manifestation of such errors, although the errors are still rather small for that case. This latter situation also implies that assuming the crack opening displacements are independent of crack size will introduce errors.

Such good agreement is not expected for sample geometries with a strongly changing weight function at small crack extensions (e.g., combined notch/crack problems); however, in the case of ceramics with very steep R-curves, the approximations do exhibit the characteristic features of the exact solution. This has been shown using an R-curve for MgLa-SN resulting from a test on a notched bending bar. Thus, one must carefully consider errors introduced by the approximation methods presented here, as well as by other common simplifying assumptions, by evaluating the effects of the weight function *a priori* for the geometric parameters corresponding to the problem being solved.

Furthermore, despite the possible errors discussed above, *in any situation* the derived first- or second-order estimates may be used to establish a starting solution of the bridging stresses for the more rigorous numerical procedure according to Ref. 7.

## Acknowledgements

JJK and SEG would like to acknowledge support from the National Science Foundation CAREER award #0547394. We also would like to thank the Deutsche Forschungsgemeinschaft DFG for financing parts of this work within the SFB 483.

## References

1. Munz D. What can we learn from R-curve measurements? *J Am Ceram Soc* 2007;**90**:1–15.
2. Fett T. Friction-induced bridging effects caused by the T-stress. *Eng Fract Mech* 1998;**59**:599–606.
3. Pezzotti G, Muraki N, Maeda N, Satou K, Nishida T. In situ measurement of bridging stresses in toughened silicon nitride using Raman microprobe spectroscopy. *J Am Ceram Soc* 1999;**82**:1249–56.
4. Pezzotti G, Ichimaru H, Ferroni L. Raman microprobe evaluation of bridging stresses in highly anisotropic silicon nitride. *JACS* 2001;**84**(8):1785–90.
5. Kruzic JJ, Cannon RM, Ager III JW, Ritchie RO. Fatigue threshold R-curves for predicting reliability of ceramics under cyclic loading. *Acta Mater* 2005;**53**:2595–605.
6. Fett T, Munz D, Kounga Njiwa AB, Rödel J, Quinn GD. Bridging stresses in sintered reaction-bonded $Si_3N_4$ from COD measurements. *J Eur Ceram Soc* 2005;**25**:29–36.
7. Fett T, Munz D, Thun G, Bahr HA. Evaluation of bridging parameters in $Al_2O_3$ from R-curves by use of the fracture mechanical weight function. *J Am Ceram Soc* 1995;**78**:949–51.
8. *Harwell Program Library*, *Subroutine V02AD*. AERE Harwell, Didcot, Oxon, UK.
9. Fett T, Fünfschilling S, Hoffmann MJ, Oberacker R, Jelitto H, Schneider GA. R-curve determination for the initial stage of crack extension in $Si_3N_4$. *J Am Ceram Soc* 2008;**91**:3638–42.
10. Fett T, Munz D. *Stress Intensity Factors and Weight Functions*. Southampton, UK: Computational Mechanics Publications; 1997.